Prospective Evaluation of ^{68}Ga-RM2 PET/MRI in Patients with Biochemical Recurrence of Prostate Cancer and Negative Findings on Conventional Imaging

Ryogo Minamimoto[1], Ida Sonni[1], Steven Hancock[2], Shreyas Vasanawala[3], Andreas Loening[3], Sanjiv S. Gambhir[4–6], and Andrei Iagaru[1]

[1]Division of Nuclear Medicine and Molecular Imaging, Department of Radiology, Stanford University, Stanford, California; [2]Department of Radiation Oncology, Stanford University, Stanford, California; [3]Radiological Sciences Laboratory, Department of Radiology, Stanford University, Stanford, California; [4]Department of Radiology, Stanford University, Stanford, California; [5]Department of Bioengineering, Stanford University, Stanford, California; and [6]Department of Materials Science and Engineering, Stanford University, Stanford, California

^{68}Ga-labeled DOTA-4-amino-1-carboxymethyl-piperidine-D-Phe-Gln-Trp-Ala-Val-Gly-His-Sta-Leu-NH_2 (^{68}Ga-RM2) is a synthetic bombesin receptor antagonist that targets gastrin-releasing peptide receptor (GRPr). GRPr proteins are highly overexpressed in several human tumors, including prostate cancer (PCa). We present data from the use of ^{68}Ga-RM2 in patients with biochemical recurrence (BCR) of PCa and negative findings on conventional imaging. **Methods:** We enrolled 32 men with BCR of PCa, who were 59–83 y old (mean ± SD, 68.7 ± 6.4 y). Imaging started at 40–69 min (mean, 50.5 ± 6.8 min) after injection of 133.2–151.7 MBq (mean, 140.6 ± 7.4 MBq) of ^{68}Ga-RM2 using a time-of-flight–enabled simultaneous PET/MRI scanner. T1-weighted, T2-weighted, and diffusion-weighted images were acquired. **Results:** All patients had a rising level of prostate-specific antigen (PSA) (range, 0.3–119.0 ng/mL; mean, 10.1 ± 21.3 ng/mL) and negative findings on conventional imaging (CT or MRI, and a ^{99m}Tc-methylene diphosphonate bone scan) before enrollment. The observed ^{68}Ga-RM2 PET detection rate was 71.8%. ^{68}Ga-RM2 PET identified recurrent PCa in 23 of the 32 participants, whereas the simultaneous MRI scan identified findings compatible with recurrent PCa in 11 of the 32 patients. PSA velocity was 0.32 ± 0.59 ng/mL/y (range, 0.04–1.9 ng/mL/y) in patients with negative PET findings and 2.51 ± 2.16 ng/mL/y (range, 0.13–8.68 ng/mL/y) in patients with positive PET findings ($P = 0.006$). **Conclusion:** ^{68}Ga-RM2 PET can be used for assessment of GRPr expression in patients with BCR of PCa. High uptake in multiple areas compatible with cancer lesions suggests that ^{68}Ga-RM2 is a promising PET radiopharmaceutical for localization of disease in patients with BCR of PCa and negative findings on conventional imaging.

Key Words: prostate cancer; ^{68}Ga; RM2; gastrin-releasing peptide receptor (GRPr); PET/MRI

J Nucl Med 2018; 59:803–808
DOI: 10.2967/jnumed.117.197624

Up to 40% of patients with prostate cancer (PCa) develop biochemical recurrence (BCR) within 10 y after initial treatment (*1*). A detectable or rising prostate-specific antigen (PSA) level after initial therapy is considered BCR, or "PSA failure," even when there are no symptoms or signs of locally recurrent or metastatic disease (*2*). Usually, an increase in the PSA level precedes clinically detectable recurrence by months to years (*3*). However, it cannot differentiate between local, regional, or systemic disease with the precision that is essential for further disease management.

Morphologic imaging methods exhibit considerable limitations: sensitivity ranges between 25% and 54% for the detection of local recurrence by transrectal ultrasound or contrast-enhanced CT and is moderately improved by using functional MRI techniques (*4*). The sensitivity of CT and MRI for detection of lymph node metastases is reported to be 30%–80% (*5*). Multiparametric MRI is improving PCa diagnosis (*6*). Using a scoring system based on a combined evaluation of diffusion-weighted imaging, dynamic contrast-enhanced imaging, and high-resolution T2-weighted imaging (*7*), the degree of suspicion on MRI strongly correlates with the presence of PCa. However, multiparametric MRI has limitations: about 20% of all index lesions are missed (*8*), the size of high-grade cancers is underestimated (*9*), and about 40% of men with normal MRI findings have PCa on biopsy (*10*).

Molecular imaging uses various targets to improve the detection of recurrent PCa. ^{18}F- or ^{11}C-labeled choline and ^{11}C-acetate were investigated (*11–13*). ^{18}F-FACBC was recently approved for the detection of PCa recurrence, and tracers binding to the prostate-specific membrane antigen (PSMA) continue to elicit high interest, although none are yet approved by the Food and Drug Administration. These promising agents do not detect all recurrences (*14,15*) and are not specific to PCa only (*16,17*). False-positives have also been reported (*18–20*).

Consequently, improved imaging of BCR of PCa continues to be an area of unmet clinical need. ^{68}Ga-labeled DOTA-4-amino-1-carboxymethyl-piperidine-D-Phe-Gln-Trp-Ala-Val-Gly-His-Sta-Leu-NH_2 (^{68}Ga-RM2) is a synthetic bombesin receptor antagonist that targets gastrin-releasing peptide receptor (GRPr) (*21*). GRPr is highly overexpressed in several human tumors, including PCa (*22*), and has been detected in 63%–100% of PCa (*23,24*). Because of the low expression of GRPr in benign prostate hypertrophy and

Received Jun. 15, 2017; revision accepted Oct. 6, 2017.
For correspondence or reprints contact: Andrei Iagaru, Division of Nuclear Medicine and Molecular Imaging, Department of Radiology, Stanford University, 300 Pasteur Dr., Room H-2200, Stanford, CA 94305.
E-mail: aiagaru@stanford.edu
Published online Oct. 30, 2017.

inflammation (*24*), imaging of GRPr has potential advantages. In a first pilot study comparing ^{68}Ga-RM2 with ^{68}Ga-PSMA-11 in PCa, both compounds performed well (*25*).

PET/MRI is an advanced technology that provides both biologic and morphologic information, with improvements over PET/CT due to better soft-tissue contrast (*26*). In this study, we evaluated ^{68}Ga-RM2 in patients with BCR of PCa and negative findings on conventional imaging, using a state-of-the-art time-of-flight–enabled simultaneous PET/MRI scanner.

MATERIALS AND METHODS

Study Population

The local Institutional Review Board and the Stanford Cancer Institute Scientific Review Committee approved the protocol (ClinicalTrials.gov identifier NCT02624518). Written informed consent was obtained from all patients before they participated in the study.

To be included in the study, the participants had to meet 5 criteria. The first was biopsy-proven PCa, and the second was a rising PSA level after definitive therapy with either radical prostatectomy or radiation therapy (external-beam or brachytherapy). If the definitive therapy had been radical prostatectomy (the American Urological Association recommendation (*27*)), the PSA level had to be at least 0.2 ng/mL—either in 1 measurement at least 6 wk after prostatectomy or persistent 2 measurements >0.2 ng/mL, the first taken at least 6 wk after surgery. If the definitive therapy had been radiation (American Society for Radiation Oncology–Phoenix consensus definition (*28*)), the PSA level had to have risen by at least 2 ng/mL over the nadir. The third inclusion criterion was no evidence of metastatic disease on conventional imaging, including a bone scan negative for skeletal metastasis and negative findings on contrast-enhanced CT or MRI. The fourth criterion was the ability to provide written consent, and the fifth was a Karnofsky performance status of at least 50 (or the Eastern Cooperative Oncology Group/World Health Organization equivalent).

Patients were excluded from participation in the study if they were less than 18 y old at the time of radiotracer administration; could not provide informed consent, lie still for the entire imaging time, or complete any of the required investigational or standard-of-care imaging examinations (e.g., severe claustrophobia or radiation phobia); had any medical condition, serious intercurrent illness, or other extenuating circumstance that the investigator believed might significantly interfere with study compliance; or had metallic implants (contraindicated for MRI).

Preparation of ^{68}Ga-RM2

The precursor, DOTA-4-amino-1-carboxymethylpiperidine-D-Phe-Gln-Trp-Ala-Val-Gly-His-Sta-Leu-NH_2 (DOTA-RM2), was obtained from ABX GmbH. A ^{68}Ga-labeling kit including eluent (concentrated NaCl/HCl solution), sodium acetate reaction buffer, ethanol (50% in water), and saline (0.9%) was obtained from Eckert and Ziegler Eurotope GmbH. Phosphate buffer concentrate (1 M Na^+, 0.6 M PO_4^{3-}) for pH adjustment was obtained from B. Braun.

The radiosynthesis was conducted with a fully automated synthesis device (Modular Lab PharmTracer; Eckert and Ziegler Eurotope GmbH) using sterile single-use cassettes, as previously reported (*25*).

PET/MRI Protocol

No specific patient preparation such as fasting or hydration was required before the ^{68}Ga-RM2 scans. Imaging (vertex to mid thighs) began 40–69 min (mean ± SD, 50.5 ± 6.8 min) after injection of 133.2–151.7 MBq (mean, 140.6 ± 7.4 MBq) of ^{68}Ga-RM2 using a time-of-flight–enabled simultaneous PET/MRI scanner (SIGNA PET/MR; GE Healthcare). The range of time from injection to start of imaging was similar to guideline recommendations for other radiopharmaceuticals evaluating PCa (*29*). The scan duration, which directly relates to the patient's height, ranged from 39 to 141 min (mean, 76.1 ± 17.4 min). Patient height ranged from 163 to 185 cm (5 ft 4 in to 6 ft 1 in) as detailed in Supplemental Table 1 (supplemental materials are available at http://jnm.snmjournals.org). In addition, one patient could not tolerate the entire examination. The PET acquisition was performed in 3-dimensional mode at 4 min/bed position (89 slices per bed position) for 5–9 bed positions. An axial 2-point Dixon 3-dimensional T1-weighted spoiled gradient-echo MR sequence was acquired at each bed position and used for generation of attenuation correction maps and for anatomic registration of the PET images. PET images were reconstructed using ordered-subset expectation maximization with 2 iterations and 28 subsets. Time-of-flight–reconstructed images assumed a gaussian kernel of 400-ps width. The Dixon MRI sequence and the PET acquisition started at the same bed position and times, thus ensuring optimal temporal and regional correspondence between the MRI and PET data. For attenuation correction, the images were segmented into different tissue types with an anatomy-aware algorithm and were coregistered to a CT atlas in the head region (*30*).

Also acquired at each bed position were a coronal T2-weighted single-shot fast spin-echo sequence with variable refocusing flip angles and outer volume suppression (*31*), a coronal diffusion-weighted sequence, and an axial T1-weighted 2-point Dixon 3-dimensional spoiled gradient-echo sequence. Spectral inversion at fat suppression was applied at every other

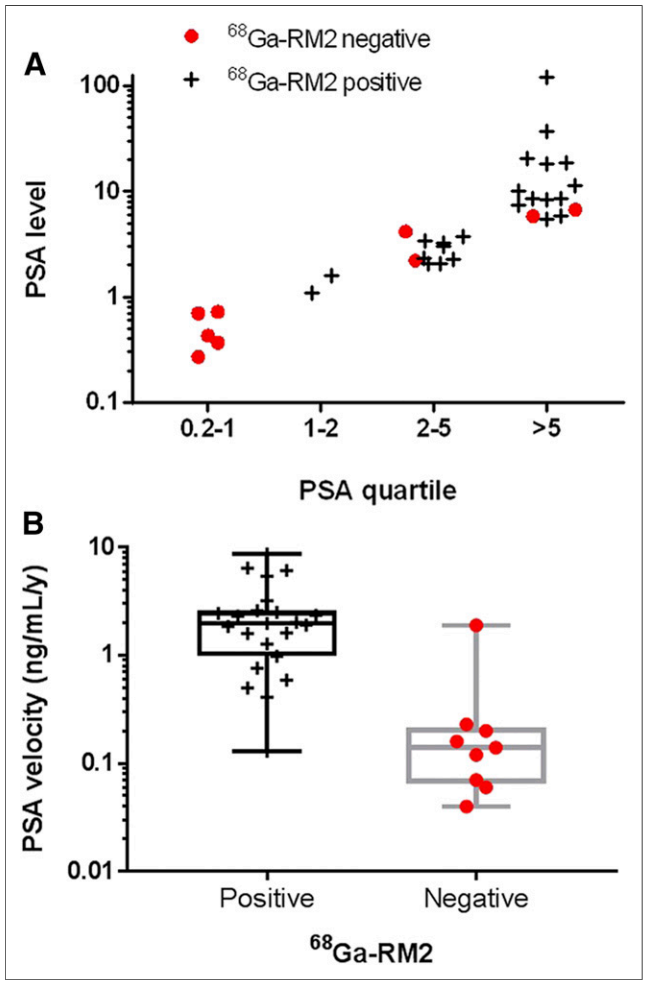

FIGURE 1. Relationship between results of ^{68}Ga-RM2 PET and PSA level (81% of patients with PSA > 1 ng/mL had positive scan findings) (A) or PSA velocity (B).

station. Because of the large prescribed field of view, each acquisition covered 2 consecutive bed positions, allowing T2-weighted whole-body images with and without fat suppression to be retrospectively generated. Coronal diffusion-weighted imaging was performed using a custom-developed 2-dimensional single-shot echo-planar imaging sequence, with 2-dimensional spatial selectivity obtained by replacing the conventional spectral–spatial excitation pulse with a 2-dimensional radiofrequency pulse. T1-weighted images were acquired using an axial 2-point Dixon 3-dimensional gradient-echo sequence (LAVA Flex) provided by the manufacturer. In the thorax region, the MRI scans were acquired during a breath-hold in shallow inspiration except for diffusion-weighted imaging, which was always performed during free breathing.

Image Analysis

Two board-certified nuclear medicine physicians with 12 and 7 y of experience in interpreting PET studies reviewed the PET images using MIMvista, version 6.2 (MIMvista Corp.). All areas of increased radiotracer uptake in sites not expected to show physiologic accumulation were reported as abnormal. Increased uptake was defined as a focus of uptake higher than uptake in the adjacent background. ^{68}Ga-RM2 uptake in the gastrointestinal tract, liver, spleen, pancreas, kidneys, ureters, and bladder was considered physiologic. This approach is similar to recently published guidelines for standard ^{68}Ga-PSMA image interpretation (*32*). The PET Edge tool available in the software was used for evaluation of focal ^{68}Ga-RM2 uptake outside the expected biodistribution. The diameters of anatomic structures corresponding to focal ^{68}Ga-RM2 uptake were measured on T1-weighted MR images.

Two board-certified radiologists (5 and 11 y of experience in interpreting body MRI studies), masked to the results of PET or other studies, evaluated the MR images for areas of abnormal signal and for abnormal anatomic structures. The criteria for detecting a lesion were visual conspicuity against the background on the diffusion-weighted images and an anatomically corresponding abnormality on the T1- and T2-weighted images.

RESULTS

We enrolled 32 men with BCR of PCa, who were 59–83 y old (mean, 68.7 ± 6.4 y). Before enrollment, they had shown negative findings on multiple standard-of-care imaging studies (CT, MRI, ^{18}F-NaF PET/CT, and ^{99m}Tc-methylene diphosphonate bone scanning, as shown in Supplemental Table 1) despite PSA levels that had risen from the nadir. The order of the standard-of-care imaging studies was not controlled, and the interval between bone scanning and anatomic imaging ranged from 0 to 28 d (mean, 3.5 ± 7.1 d). The time from conventional imaging to enrollment ranged from 1 to 45 d (mean, 26.7 ± 12.7 d). The patients did not receive treatment during this interval. The interval from BCR to the ^{68}Ga-RM2 PET/MRI scan ranged from 1 to 75 mo (mean, 21.8 ± 19.5 d).

The patient characteristics are shown in Supplemental Table 1, and the PET/MRI results and follow-up data are shown in Supplemental Table 2. The patients were not being treated for PCa at the time of enrollment. All tolerated the procedure without immediate or delayed (≤7 d) complaints or complications. The biodistribution of ^{68}Ga-RM2 was similar to previous reports (*33,34*).

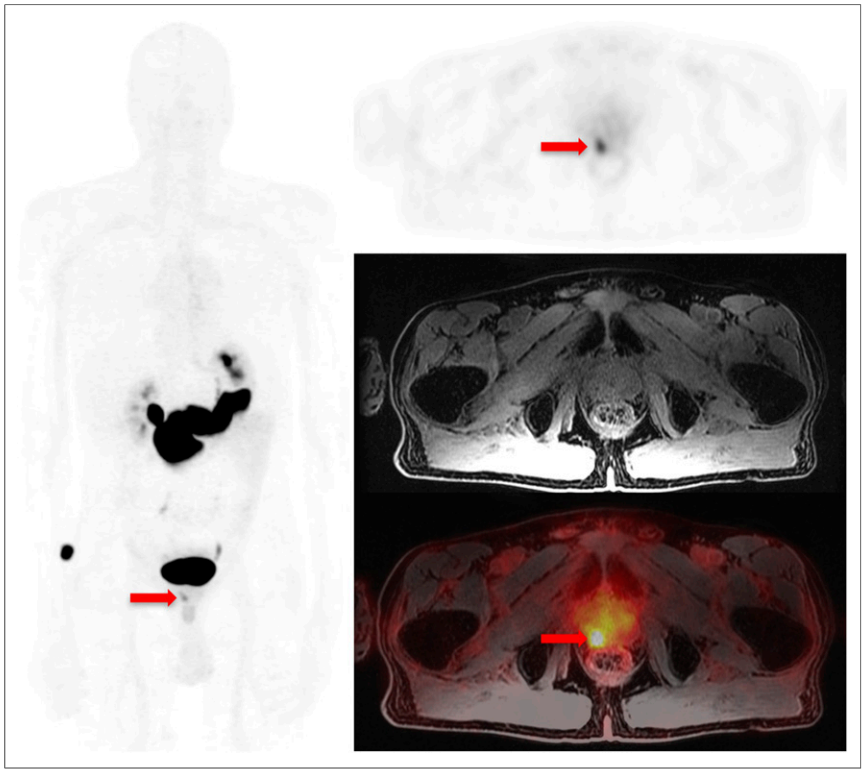

FIGURE 2. A 72-y-old man (participant 6) with PCa treated with radiation therapy and androgen deprivation therapy at initial presentation (Gleason score, 3 + 4), now with BCR since 2013 and rising PSA level (from 0.21 ng/mL initially to 3.7 ng/mL at time of scan). Maximum-intensity projection (left) and transaxial (top right) ^{68}Ga-RM2 PET images show focal uptake (arrows) corresponding to prostate bed on T1-weighted MRI (middle right) and fused PET/MRI (bottom right). Focal uptake in prostate bed was confirmed by biopsy to represent recurrent adenocarcinoma.

^{68}Ga-RM2 Uptake Outside the Expected Physiologic Biodistribution

Nine scans had no focal ^{68}Ga-RM2 uptake outside the expected physiologic biodistribution. The remaining 23 scans had high focal ^{68}Ga-RM2 uptake that corresponded on MRI to retroperitoneal lymph nodes, bone marrow, mediastinal lymph nodes, pelvic lymph nodes, seminal vesicle, supraclavicular lymph nodes, mesenteric lymph nodes, liver, lung, or prostate bed. These areas of high ^{68}Ga-RM2 uptake had an SUV_{max} of 13.4 ± 8.3 (range, 2.6–33.5) and an SUV_{mean} of 6.7 ± 3.9 (range, 1.7–16.1) above the background and were easily identifiable given the minimal hepatobiliary clearance. The mean diameter of lymph nodes with high ^{68}Ga-RM2 uptake was 1.3 ± 0.8 cm (range, 0.4–2.9 cm).

The participants were followed for an average of 17.1 ± 5.2 mo (range, 3–25 mo) after the ^{68}Ga-RM2 scan. Of the 23 participants with findings on ^{68}Ga-RM2 PET, 20 began treatment. Two participants continued active surveillance, and a third declined the offered treatment. Seven of the 23 ^{68}Ga-RM2–positive cases had biopsies that confirmed the PET findings. Conversely, of the 9 participants with no findings on ^{68}Ga-RM2 PET, 6 continued on active surveillance, 2 received treatment, and 1 was lost to follow-up. Participants with findings on ^{68}Ga-RM2

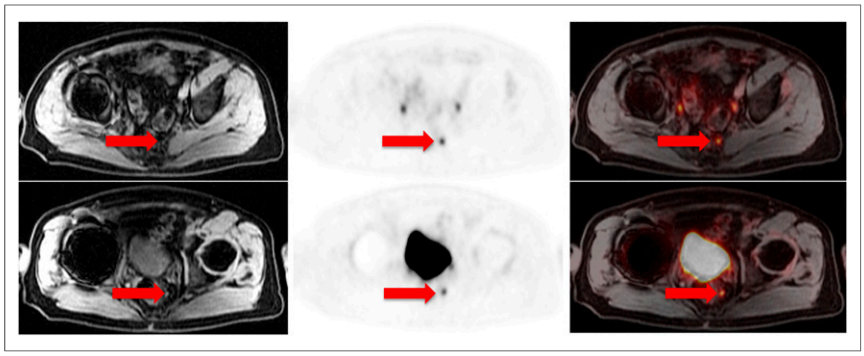

FIGURE 3. A 65-y-old man (participant 11) with PCa treated with radical prostatectomy at initial presentation (Gleason score, 4 + 3), now with BCR since 2015 and rising PSA level (from 0.45 ng/mL initially to 2.33 ng/mL at time of scan). Transaxial ^{68}Ga-RM2 PET images (middle) show focal uptake (arrows) corresponding to <5-mm pelvic lymph nodes on T1-weighted MRI (left) and fused PET/MRI (right). PSA level decreased to <0.05 ng/mL after pelvic radiation therapy targeting these lymph nodes.

PET who underwent immediate active treatment generally had a decrease in their PSA level, whereas participants who initially remained under observation had an increase in their PSA level and started treatment. All these details are presented in Supplemental Table 2.

Relationship Between PSA Level and Scan Results

PSA levels were sampled at 21.4 ± 10.8 d (range, 1–30 d) before the scan and measured 10.1 ± 21.3 ng/mL (range, 0.3–119.0 ng/mL). In patients with negative PET findings, the PSA level was 2.4 ± 2.5 ng/mL (range, 0.3–6.7 ng/mL), and in patients with positive PET findings, the PSA level was 13.2 ± 24.5 ng/mL (range, 1.1–119.0 ng/mL). This difference was not statistically significant (P = 0.20). Figure 1 shows the relationship of scan positivity to PSA level and PSA velocity.

Relationship Between PSA Velocity and Scan Results

PSA velocity measured 1.89 ± 2.1 ng/mL/y (range, 0.04–8.68 ng/mL/y): 0.32 ± 0.59 ng/mL/y (range, 0.04–1.9 ng/mL/y) in patients with negative PET findings and 2.51 ± 2.16 ng/mL/y (range, 0.13–8.68 ng/mL/y) in patients with positive PET findings. This difference was statistically significant (P = 0.006). Of the 9 patients with negative ^{68}Ga-RM2 findings, only 1 patient had a PSA velocity greater than 0.3 ng/mL/y.

MRI Findings

Eleven of the 32 participants had findings compatible with recurrent PCa on the MRI component of PET/MRI. These findings included lesions in the lymph nodes, prostate bed, lung, and bone marrow. All were also positive on ^{68}Ga-RM2 PET. The remaining 21 participants had no abnormal findings identified prospectively.

Examples of recurrent PCa are shown in Figures 2–5.

DISCUSSION

To the best of our knowledge, our study was the largest to date to prospectively evaluate ^{68}Ga-RM2 in a series of patients with BCR of PCa. In this population, with a mean PSA level of 10.1 ng/mL, the detection rate observed on ^{68}Ga-RM2 PET was 71.8%. ^{68}Ga-RM2 PET/MRI showed intense uptake in multiple subcentimeter-sized pelvic, retroperitoneal, and mesenteric lymph nodes and in lesions of the prostate bed, seminal vesicle, lung, liver, and bone marrow that had not been identified on conventional imaging before enrollment. However, some of the lesions, such as lung nodules, were outside the standard field of view for restaging of PCa using anatomic imaging. The high uptake in the pancreas and moderate uptake in the gastrointestinal tract are specific features of ^{68}Ga-RM2 biodistribution. The pancreas and gastrointestinal tract express GRPr (*35*), and bombesin stimulates pancreatic secretion, as well as gastrin and cholecystokinin release (*36,37*). ^{68}Ga-RM2 PET identified recurrent PCa in 23 of the 32 participants (71%), whereas the simultaneous MRI scan identified findings compatible with recurrent PCa in only 11 of the 32 participants (34%). Of the 9 ^{68}Ga-RM2–negative patients, 2 had no evidence of disease during the follow-up period, 1 was lost to follow-up and determination of clinical disease was not possible, and 6 had false-negative findings with subsequent clinical disease. The percentage of patients with a correct diagnosis (compared with clinical outcome) was 80.1% (25/31). The confirmed false-negatives were thus 16.1% (5/31). All patients false-negative on ^{68}Ga-RM2 were also false-negative on MRI. There were no patients with clinical disease who had positive MRI findings and negative ^{68}Ga-RM2 findings.

The statistically significant difference in mean PSA velocity between patients negative on ^{68}Ga-RM2 PET (0.32 ± 0.59 ng/mL/y; median, 0.14 ng/mL/y) and patients positive on ^{68}Ga-RM2 PET (2.51 ± 2.16 ng/mL/y; median, 1.95 ng/mL/y) reveals a

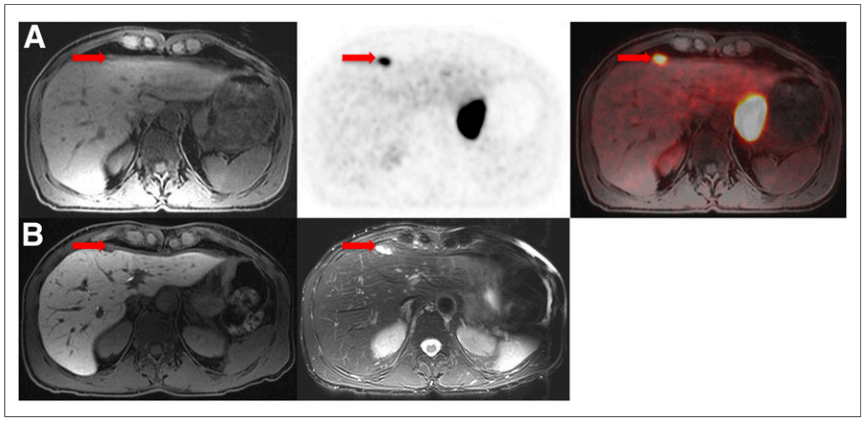

FIGURE 4. A 65-y-old man (participant 23) with PCa treated with radical prostatectomy, radiation therapy, and androgen blockade at initial presentation (Gleason score, 3 + 5), now with BCR since 2014 and rising PSA level (from 0.72 ng/mL initially to 3.4 ng/mL at time of scan). (A) Transaxial ^{68}Ga-RM2 PET image (middle) shows focal uptake (arrows) corresponding to liver capsule on MRI (T1-weighted, left) and fused PET/MRI (right). MRI did not identify anatomic lesion. (B) Follow-up MRI (left: T1-weighted; right: T2-weighted) done 4 mo later shows lesion (arrows), which was biopsy-proven to represent metastatic adenocarcinoma of prostate origin.

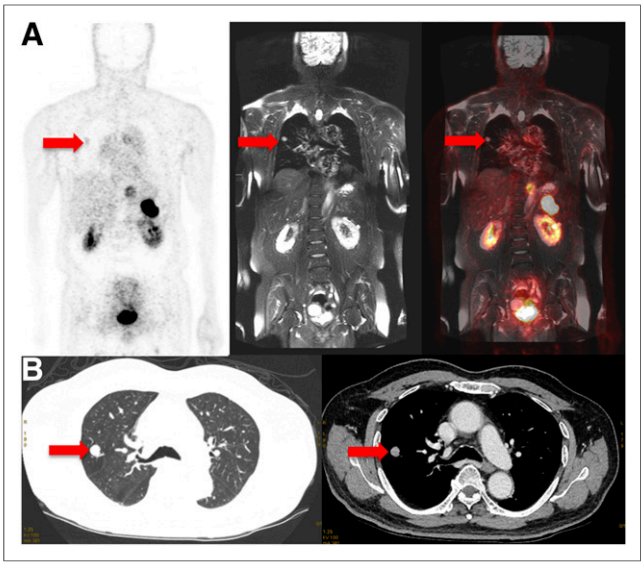

FIGURE 5. A 66-y-old man (participant 20) with PCa treated with surgery, radiation therapy, and androgen deprivation therapy at initial presentation (Gleason score, 5 + 4), now with BCR since 2010 and rising PSA level (from 0.07 ng/mL initially to 10.1 ng/mL at time of scan). (A) Coronal ^{68}Ga-RM2 PET image (left) shows faint (but greater than in adjacent normal lung parenchyma) focal uptake (arrows) corresponding to lung nodule on T2-weighted MRI (middle) and fused PET/MRI (right). (B) Follow-up dedicated chest CT done 2 wk later shows lung nodule (arrows), which was biopsy-proven to represent metastatic adenocarcinoma of prostate origin.

difference in pathology and potential prognosis and indicates that PSA velocity may be a tool to decide which patients may show positivity. The mean PSA velocity in patients positive on ^{68}Ga-RM2 PET was greater than 2 ng/mL/y, which has been shown to be significantly associated with a decreased time to PCa-specific and all-cause mortality, compared with 2.0 ng/mL/y or less (*38*). If corroborated in a larger study, negative ^{68}Ga-RM2 findings, even in the face of an elevated PSA level, may indicate a patient with a relatively benign prognosis for whom a watch-and-wait strategy is indicated. Our preliminary follow-up data shown in Supplemental Table 2 support this hypothesis.

To date, only 3 studies have reported the performance of ^{68}Ga-RM2 PET in BCR of PCa. Kähkönen et al. evaluated ^{68}Ga-RM2 using PET/CT in 14 men with PCa; however, 11 of the 14 participants were scanned for evaluation at initial diagnosis, and only 3 of the 14 were scanned at BCR. In that study, the sensitivity was 88% for detection of primary PCa and 70% for detection of lymph node metastases (*34*). Other GRPr-targeting PET radiopharmaceuticals have recently been reported in small cohorts, illustrating the attractiveness of this target for detection of PCa. Maina et al. evaluated ^{68}Ga-SB3 in 8 patients with breast cancer and 9 patients with PCa (*39*). ^{68}Ga-SB3 did not produce adverse effects and identified cancer lesions in 4 of 8 patients (50%) with breast cancer and 5 of 9 patients (55%) with PCa. An improved version of this radiopharmaceutical, ^{68}Ga-NeoBOMB1, is showing promising results in preliminary studies (*40,41*).

In our study, ^{68}Ga-RM2 showed high focal uptake in small lymph nodes that had no MRI features compatible with metastatic disease. Future larger studies will compare ^{68}Ga-RM2 with multiparametric MRI or one of the new PSMA PET radiopharmaceuticals for the detection of metastatic PCa. The high performance of the time-of-flight–enabled PET/MRI scanner (*30*) likely contributed to the identification of focal ^{68}Ga-RM2 uptake in structures of nonpathologically increased size but outside the expected physiologic ^{68}Ga-RM2 biodistribution. However, if there is no concern about pelvic recurrence, PET/CT is likely to yield results similar to PET/MRI with shorter imaging times, especially when using the recently introduced silicon-photomultiplier–based PET/CT scanners (*42*).

One limitation of our study was the small number of patients. Another was the lack of correlation with pathology results for all patients. However, of the 23 patients with findings on ^{68}Ga-RM2 PET, pathology results were available for 7, all of whom were confirmed to have recurrent PCa. In addition, given the small size of many of the lymph nodes with focal uptake, accurate sampling would not have been feasible in all cases. A third limitation—which is expected in early evaluations of new radiopharmaceuticals—was the heterogeneity in PSA levels and prior treatment regimens at enrollment. Subsequent studies will investigate more homogeneous patient populations.

CONCLUSION

We successfully used ^{68}Ga-RM2 PET in a prospective study to detect PCa lesions in patients with BCR of PCa and negative findings on conventional imaging. High focal uptake in putative and biopsy-proven sites of recurrent PCa in 23 of the 32 participants was observed using time-of-flight–enabled simultaneous PET/MRI, and ^{68}Ga-RM2 PET detected more lesions than MRI alone. Therefore, we propose ^{68}Ga-RM2 as a promising PET radiopharmaceutical for localization of disease in such patients. Future work should explore the role of ^{68}Ga-RM2 in relationship to widely adopted PSMA PET radiopharmaceuticals such as ^{68}Ga-PSMA-11.

DISCLOSURE

The precursor and reference compound were provided by Piramal Imaging, GmbH. No other potential conflict of interest relevant to this article was reported.

ACKNOWLEDGMENTS

We thank Dawn Banghart, George Segall, and the other members of the Radioactive Drug Research Committee for advice and support. We also thank our research coordinators, Pam Gallant and Krithika Rupnarayan; the Cyclotron and Radiochemistry Facility; the nuclear medicine technologists; and all the patient participants and their families.

REFERENCES

1. Isbarn H, Wanner M, Salomon G, et al. Long-term data on the survival of patients with prostate cancer treated with radical prostatectomy in the prostate-specific antigen era. *BJU Int.* 2010;106:37–43.
2. D'Amico AV, Whittington R, Malkowicz SB, et al. Pretreatment nomogram for prostate-specific antigen recurrence after radical prostatectomy or external-beam radiation therapy for clinically localized prostate cancer. *J Clin Oncol.* 1999; 17:168–172.
3. Van Poppel H, Vekemans K, Da Pozzo L, et al. Radical prostatectomy for locally advanced prostate cancer: results of a feasibility study (EORTC 30001). *Eur J Cancer.* 2006;42:1062–1067.
4. Beer AJ, Eiber M, Souvatzoglou M, Schwaiger M, Krause BJ. Radionuclide and hybrid imaging of recurrent prostate cancer. *Lancet Oncol.* 2011;12:181–191.
5. Oyen RH, Van Poppel HP, Ameye FE, Van de Voorde WA, Baert AL, Baert LV. Lymph node staging of localized prostatic carcinoma with CT and CT-guided fine-needle aspiration biopsy: prospective study of 285 patients. *Radiology.* 1994;190:315–322.

6. Johnson LM, Turkbey B, Figg WD, Choyke PL. Multiparametric MRI in prostate cancer management. *Nat Rev Clin Oncol.* 2014;11:346–353.
7. Steiger P, Thoeny HC. Prostate MRI based on PI-RADS version 2: how we review and report. *Cancer Imaging.* 2016;16:9.
8. Le JD, Tan N, Shkolyar E, et al. Multifocality and prostate cancer detection by multiparametric magnetic resonance imaging: correlation with whole-mount histopathology. *Eur Urol.* 2015;67:569–576.
9. Priester A, Natarajan S, Khoshnoodi P, et al. Magnetic resonance imaging underestimation of prostate cancer geometry: use of patient specific molds to correlate images with whole mount pathology. *J Urol.* 2017;197:320–326.
10. Sonn GA, Chang E, Natarajan S, et al. Value of targeted prostate biopsy using magnetic resonance-ultrasound fusion in men with prior negative biopsy and elevated prostate-specific antigen. *Eur Urol.* 2014;65:809–815.
11. Sandblom G, Sorensen J, Lundin N, Haggman M, Malmstrom PU. Positron emission tomography with C11-acetate for tumor detection and localization in patients with prostate-specific antigen relapse after radical prostatectomy. *Urology.* 2006;67:996–1000.
12. Oyama N, Miller TR, Dehdashti F, et al. ^{11}C-acetate PET imaging of prostate cancer: detection of recurrent disease at PSA relapse. *J Nucl Med.* 2003;44:549–555.
13. Wachter S, Tomek S, Kurtaran A, et al. ^{11}C-acetate positron emission tomography imaging and image fusion with computed tomography and magnetic resonance imaging in patients with recurrent prostate cancer. *J Clin Oncol.* 2006; 24:2513–2519.
14. Eiber M, Maurer T, Souvatzoglou M, et al. Evaluation of hybrid ^{68}Ga-PSMA ligand PET/CT in 248 patients with biochemical recurrence after radical prostatectomy. *J Nucl Med.* 2015;56:668–674.
15. Rowe SP, Gage KL, Faraj SF, et al. ^{18}F-DCFBC PET/CT for PSMA-based detection and characterization of primary prostate cancer. *J Nucl Med.* 2015; 56:1003–1010.
16. Sathekge M, Lengana T, Modiselle M, et al. ^{68}Ga-PSMA-HBED-CC PET imaging in breast carcinoma patients. *Eur J Nucl Med Mol Imaging.* 2017;44:689–694.
17. Rhee H, Blazak J, Tham CM, et al. Pilot study: use of gallium-68 PSMA PET for detection of metastatic lesions in patients with renal tumour. *EJNMMI Res.* 2016;6:76.
18. Hermann RM, Djannatian M, Czech N, Nitsche M. Prostate-specific membrane antigen PET/CT: false-positive results due to sarcoidosis? *Case Rep Oncol.* 2016;9:457–463.
19. Sasikumar A, Joy A, Nanabala R, Pillai MR, TA H. ^{68}Ga-PSMA PET/CT false-positive tracer uptake in Paget disease. *Clin Nucl Med.* 2016;41:e454–e455.
20. Noto B, Vrachimis A, Schafers M, Stegger L, Rahbar K. Subacute stroke mimicking cerebral metastasis in ^{68}Ga-PSMA-HBED-CC PET/CT. *Clin Nucl Med.* 2016;41:e449–e451.
21. Jensen RT, Battey JF, Spindel ER, Benya RV. International Union of Pharmacology: LXVIII—mammalian bombesin receptors: nomenclature, distribution, pharmacology, signaling, and functions in normal and disease states. *Pharmacol Rev.* 2008;60:1–42.
22. Reubi JC, Wenger S, Schmuckli-Maurer J, Schaer J-C, Gugger M. Bombesin receptor subtypes in human cancers: detection with the universal radioligand ^{125}I-[D-TYR6, β-ALA11, PHE13, NLE14] bombesin(6–14). *Clin Cancer Res.* 2002;8:1139–1146.
23. Sun B, Halmos G, Schally AV, Wang X, Martinez M. Presence of receptors for bombesin/gastrin-releasing peptide and mRNA for three receptor subtypes in human prostate cancers. *Prostate.* 2000;42:295–303.
24. Markwalder R, Reubi JC. Gastrin-releasing peptide receptors in the human prostate: relation to neoplastic transformation. *Cancer Res.* 1999;59:1152–1159.
25. Minamimoto R, Hancock S, Schneider B, et al. Pilot comparison of ^{68}Ga-RM2 PET and ^{68}Ga-PSMA-11 PET in patients with biochemically recurrent prostate cancer. *J Nucl Med.* 2016;57:557–562.
26. Antoch G, Bockisch A. Combined PET/MRI: a new dimension in whole-body oncology imaging? *Eur J Nucl Med Mol Imaging.* 2009;36(suppl 1):S113–S120.
27. Cookson MS, Aus G, Burnett AL, et al. Variation in the definition of biochemical recurrence in patients treated for localized prostate cancer: the American Urological Association Prostate Guidelines for Localized Prostate Cancer Update Panel report and recommendations for a standard in the reporting of surgical outcomes. *J Urol.* 2007;177:540–545.
28. Roach M III, Hanks G, Thames H Jr, et al. Defining biochemical failure following radiotherapy with or without hormonal therapy in men with clinically localized prostate cancer: recommendations of the RTOG-ASTRO Phoenix Consensus Conference. *Int J Radiat Oncol Biol Phys.* 2006;65:965–974.
29. Fendler WP, Eiber M, Beheshti M, et al. ^{68}Ga-PSMA PET/CT: joint EANM and SNMMI procedure guideline for prostate cancer imaging—version 1.0. *Eur J Nucl Med Mol Imaging.* 2017;44:1014–1024.
30. Iagaru A, Mittra E, Minamimoto R, et al. Simultaneous whole-body time-of-flight ^{18}F-FDG PET/MRI: a pilot study comparing SUVmax with PET/CT and assessment of MR image quality. *Clin Nucl Med.* 2015;40:1–8.
31. Loening AM, Saranathan M, Ruangwattanapaisarn N, Litwiller DV, Shimakawa A, Vasanawala SS. Increased speed and image quality in single-shot fast spin echo imaging via variable refocusing flip angles. *J Magn Reson Imaging.* 2015;42:1747–1758.
32. Fanti S, Minozzi S, Morigi JJ, et al. Development of standardized image interpretation for ^{68}Ga-PSMA PET/CT to detect prostate cancer recurrent lesions. *Eur J Nucl Med Mol Imaging.* 2017;44:1622–1635.
33. Roivainen A, Kahkonen E, Luoto P, et al. Plasma pharmacokinetics, whole-body distribution, metabolism, and radiation dosimetry of ^{68}Ga bombesin antagonist BAY 86-7548 in healthy men. *J Nucl Med.* 2013;54:867–872.
34. Kähkönen E, Jambor I, Kemppainen J, et al. In vivo imaging of prostate cancer using [^{68}Ga]-labeled bombesin analog BAY86-7548. *Clin Cancer Res.* 2013;19: 5434–5443.
35. Nishino H, Tsunoda Y, Owyang C. Mammalian bombesin receptors are coupled to multiple signal transduction pathways in pancreatic acini. *Am J Physiol.* 1998;274:G525–G534.
36. Polak JM, Bloom SR, Hobbs S, Solcia E, Pearse AG. Distribution of a bombesin-like peptide in human gastrointestinal tract. *Lancet.* 1976;1:1109–1110.
37. Erspamer V, Improta G, Melchiorri P, Sopranzi N. Evidence of cholecystokinin release by bombesin in the dog. *Br J Pharmacol.* 1974;52:227–232.
38. D'Amico AV, Renshaw AA, Sussman B, Chen MH. Pretreatment PSA velocity and risk of death from prostate cancer following external beam radiation therapy. *JAMA.* 2005;294:440–447.
39. Maina T, Bergsma H, Kulkarni HR, et al. Preclinical and first clinical experience with the gastrin-releasing peptide receptor-antagonist [^{68}Ga]SB3 and PET/CT. *Eur J Nucl Med Mol Imaging.* 2016;43:964–973.
40. Dalm SU, Bakker IL, de Blois E, et al. ^{68}Ga/^{177}Lu-NeoBOMB1, a novel radiolabeled GRPR antagonist for theranostic use in oncology. *J Nucl Med.* 2017; 58:293–299.
41. Nock BA, Kaloudi A, Lymperis E, et al. Theranostic perspectives in prostate cancer with the gastrin-releasing peptide receptor antagonist NeoBOMB1: preclinical and first clinical results. *J Nucl Med.* 2017;58:75–80.
42. Baratto L, Park SY, Hatami N, et al. ^{18}F-FDG silicon photomultiplier PET/CT: a pilot study comparing semi-quantitative measurements with standard PET/CT. *PLoS One.* 2017;12:e0178936.